Title
Measurement of plant cells and organelles using computer-enhanced digitally processed images

Journal
Environmental and Experimental Botany, 27(2)

ISSN
0098-8472

Authors
Walter, RJ
Berns, MW
Arditti, J
et al.

Publication Date
1987-04-01

DOI
10.1016/0098-8472(87)90068-2

Environmental and Experimental Botany, Vol. 27, No. 2, pp. 177 to 184, 1987.
Printed in Great Britain.

0098-8472/87 $3.00 + 0.00
Pergamon Journals Ltd.

MEASUREMENT OF PLANT CELLS AND ORGANELLES USING COMPUTER-ENHANCED DIGITALLY PROCESSED IMAGES

R. J. WALTER, JR., M. W. BERNS, J. ARDITTI and L. P. NYMAN

Department of Developmental and Cell Biology, University of California, Irvine, Irvine, California 92717, U.S.A.

(*Received* 1 *April* 1986; *accepted in revised form* 1 *July* 1986)

WALTER R. J., JR., BERNS M. W., ARDITTI J. and NYMAN L. P. *Measurement of plant cells and organelles using computer-enhanced digitally processed images.* ENVIRONMENTAL AND EXPERIMENTAL BOTANY **27**, 177–184, 1987.—A computer enhanced video microscopy system can be used to study the morphometry of chloroplasts and cells of *Colocasia esculenta* var. *antiquorum*. This system is rapid and accurate, and enhances microscopic images, thereby facilitating measurements. It also introduces automation in statistical analyses.

INTRODUCTION

MORPHOMETRY involving the size and shape relationships between structures has been used in studies of plant development,[9] taxonomy and morphology.[7] Measurements for such studies are typically obtained manually, using photographic images or camera lucida drawings. These methods are tedious, and subject to errors that may affect their accuracy. Errors can arise from poor image quality and/or reproduction, as well as from human miscalculations. Computers can be used for morphometric analyses, but they are usually employed after most of the data have been gathered. These difficulties, along with the necessary statistical calculations, can be a strong deterrent.

In recent years there has been a tendency to apply computerized techniques based on video images to morphometric anaylses of biological specimens.[4,15,16] These procedures utilize digitized images stored in computer memory, and can overcome many of the difficulties associated with manual analysis. Improvements arise from three primary sources. First, the use of a video camera allows images to be displayed at 30 frames/sec, which is essentially instantaneous for most purposes. The rapid capture and display allow convenient adjustment of the system for optimal image contrast, brightness or other parameters.

Second, a high speed digitizer can convert the analog video signal into a matrix of discrete intensity values ('pixels') which are used to represent the image in computer memory. The video image is transformed into a rectangular array with up to 1024 pixels on a side, each pixel in turn may represent up to 1024 different intensity values. This digitizing process can be performed at video rates (i.e. the image can be stored in the memory of the computer as quickly as it can be produced by the video system). In contrast, manual techniques require that individual pixel values be entered through a keyboard terminal one at a time.

The third advantage of automated morphometric analysis is the use of a high speed computer with appropriate software. This makes possible rapid analysis of the stored digital image. Automated analysis is faster than manual procedures and the results are reproducible. In addition, the subjective errors inherent in manual methods can be avoided.

In this paper we describe a computerized video microscope system (Fig. 1) which can be used to analyze the morphology of plant cells and organelles.

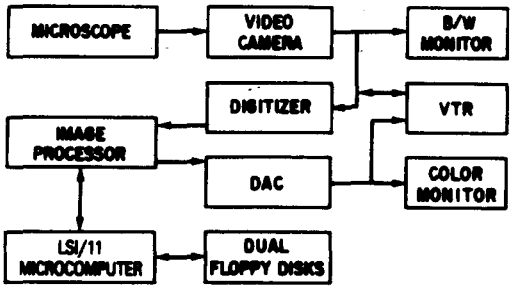

FIG. 1. Schematic diagram of the image processing system.[17] Optical images from the axiomat microscope are captured by a video camera and directed to a video digitizer with 6-bit resolution. Video images from the camera can also be directed to a monochrome display monitor or to a video tape recorder (VTR). Digitized images can be stored and processed in the DeAnza IP5500 image array processor, which is controlled by an LSI-11 minicomputer. Processed images are reconverted to video format and are displayed on a high resolution Hitachi RGB color monitor. Digitized images and other data can be stored on 8 in. floppy disks. Abbreviations: VTR = video tape recorder, DAC = digital to analog converter.

MATERIALS AND METHODS

Plant material

Tissues of taro, *Colocasia esculenta* var *antiquorum* (L) Schott., Aracreae were cultured *in vitro* on a series of seawater-containing media.[10]

Material for light microscopy was cut into segments no larger than 0.25 cm^2, fixed overnight in 4% glutaraldehyde buffered with 0.1 M sodium cacodylate (pH 7.2), and washed and dehydrated in acetone at 0°C. After that the tissues were gradually brought to room temperature, infiltrated with Spurr resin and embedded at 70°C for 18 hr. Sections 2 μm thick were cut with a JB-4 Sorvall Porter Blum microtome mounted on glass slides and stained in 0.1% aqueous toluidine blue. Slides were sealed with coverslips, using immersion oil as mounting medium. To stabilize tissues taken from samples grown in seawater-containing media, sucrose was added to the fixation solution (NYMAN and ARDITTI, unpublished).

Optics

Optical images were produced on an inverted Zeiss AXIOMAT microscope using a 25X AXIOMAT planapochromat objective and bright field optics. The microscope was equipped with a computer-controlled motorized stepping stage with 0.5 μm resolution in the X and Y directions. This stage was calibrated using a micrometer (American Optical), and found to have a displacement accuracy of better than $\pm 5\%$ over distances of several hundred micra. Optical images were projected to the video camera through a side port of the microscope (Fig. 1), and could be viewed simultaneously through the oculars.[16] Representative fields of the plant specimens were selected at random.

Video camera

Output from the video camera (Fig. 1) was digitized at video rates by a DeAnza IP5500 image arrray processor (Gould/DeAnza, San Jose, CA). Each video frame was converted into a 512×512 array of 6-bit pixels, and stored in one of the $512 \times 512 \times 8$-bit image memories. Consecutive video images were accumulated in the memory and averaged to produce an 8-bit image with relative intensity values ranging from 0 to 255. Typically 32 frames were averaged for this purpose prior to analysis. Gray values of 0 and 225 corresponded to the darkest and brightest regions of the image, respectively. The controls of the video camera and optical system were routinely adjusted to produce an image that utilized the full dynamic range of the digital memory.[2] Optimal settings for the system could be determined quickly by using the real-time processing capabilities of the image processor. Once determined, these values were not altered for each observation period.

Stored digital images were manipulated and analyzed using algorithms developed on a DEC LSI-11/23 host processor (Digital Equipment Corporation, Maynard, MA) in either FORTRAN or MACRO programming languages. Analysis consisted of (1) detection and segmentation (outlining) of chloroplast boundaries within the image, and (2) use of chain-coding algorithms to calculate statistics of area, perimeter and diameter for each chloroplast. Detection and analysis were carried out interactively.

The computer operator determined gray value threshold levels for boundary detection. These were used to complete boundary segment definitions when the distinction between chloroplast membrane and cell wall could not be established by gray value alone.

Measurements were expressed in μm and μm^2 by using calibration factors to account for the magnification of the microscope/video system. Due to sources of distortion common to most video cameras, this calibration must be determined in both the X and Y directions,[2] and may even change at different positions within the video image.[5] Calibration was performed by the computer system through use of the X and Y stepping-motors that control movement of the microscope stage. The motors were used to produce known displacements of an object in the video image. Displacement of the object within the digitized image was noted by the computer operator, using a joystick-controlled cursor to mark its position before and after the movement. The computer then calculated a calibration factor in units of μm/pixel. This procedure was followed for displacements in both the X and Y directions.

RESULTS

Image selection and optimization

Cell fields were selected randomly for analysis by scanning the image on the video monitor. Once an appropriate field was chosen, the video system was adjusted to display an image (Figs 2A and B) with optimal contrast and brightness.[2] Small imperfections in the displayed image, such as knife marks, can be removed using a gray value threshold procedure (Fig. 2B).

In this procedure, all pixels with a gray value above an arbitrary threshold are set to a new gray value equal to the background average. This procedure is useful for improving the image display but it is not required for the analytical procedure described below.

Image capture and digitizing

The video image was digitized at real-time video rates and stored in one of the image memories of the array processor. Each video image was converted into a 512×512 arrray of 6-bit picture pixels. The gray value of each pixel was linearly proportional to the amplitude of the video signal. Magnification of the optical image to the video camera was maintained in such a way that the sampling interval of the digitizer (the width of a single pixel) was generally 2–3 times smaller than the resolution limit of the microscope. This overscanning ensures that the smallest resolvable features in the optical image are reproduced in the digital image.[13]

Video images generally contain some degree of random electronic noise which appears as a grainy pattern. The effect of this noise can be reduced by accumulating and averaging multiple digital images of each microscope field. This procedure was used in the present study because it improves the signal-to-noise ratio of the digital image by a factor of $\bar{N}$, where N is the number of images averaged.[5]

Chloroplast identification and isolation

Further processing of the digital image by the computer requires that the chloroplast-containing part be isolated and identified. This identification can be achieved by a gray-value threshold technique which separates the chloroplast image from the darker background in the digital image. Under bright field optics (Fig. 3A), the chloroplasts and cell walls have high contrast and appear darker than the background areas. The difference in brightness between the chloroplasts and the background (Fig. 2 vs Fig. 3) can be used to identify them through the use of a threshold procedure that converts all pixels above a certain threshold value to a gray value of 255 (white) and all those below it to 0 (black).

This procedure relies on the principle that there are unique gray values within the image which are found only in chloroplasts or within background regions. The gray value threshold separates the distributions of these two pixel types. This makes it possible to classify image regions on the basis of gray value alone[17] and produces distinctions between chloroplast and background regions (Figs 2A, 2B and 3A) as well as a sharp peak in the gray value histogram (Fig. 3B), allowing the threshold to be set with accuracy.

In this study gray value thresholds were set interactively using a joystick device during processing and display. In most cases this procedure was successful in isolating chloroplasts found in

regions of clear cytoplasm. However some difficulty was encountered in isolating those that were in close proximity to cell walls or to other chloroplasts (Fig. 3C). This closeness results in a merging of these structures in the thresholded image (Fig. 3C), due to their similar gray values. The merging cannot be overcome by modification in the gray value threshold because there is no unique gray value that can be used to differentiate such similar structures.

When merged structures could not be differentiated on the basis of gray value thresholds, an editing function was used to define the boundaries among chloroplasts, or between them and the cell wall. This editing was carried out by drawing the missing boundary segments between merged structures with a cursor (Fig. 3D).

Image segmentation

Once chloroplasts could be identified unambiguously in the digital image, the host computer was used to automatically trace their perimeter using a boundary-following algorithm. The algorithm starts with a computer operator moving a cursor to the immediate left of the chloroplast to be measured. This identifies the object to the computer, which then searches to the right until it finds the first non-black pixel. Once this edge pixel has been identified, the computer examines neighboring pixels in order to find another edge element which is connected to the first. The criteria used for identifying additional edge elements are that the pixel must have a gray value of 255, and be adjacent to (1) at least one background pixel with a gray value of zero, and (2) a previously identified edge element.

Due to the matrix arrangement of the digital image, each pixel has only eight immediate neighbors. By convention, boundary-following algorithms can be made to search for (1) only those pixels that are connected orthogonally ('four-connected' pixels), or (2) all pixels that are connected either orthogonally or diagonally ('eight-connected' pixels; Figs 4A, B and C). Due to certain ambiguities that can arise from eight-connected object boundaries, many boundary-following routines are restricted to search for only four-connected pixels (Dr Jack Sklansky, Department of Electrical Engineering, University of California, Irvine, personal communication).

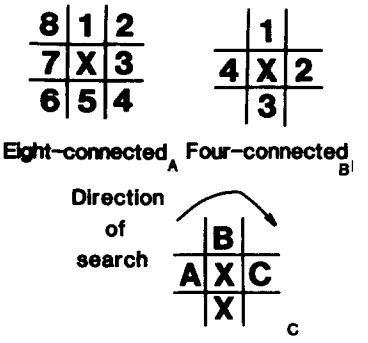

FIG. 4. Eight-pixel (A) connectivity vs four-pixel (B) connectivity. The pixel of interest (X in the figures) can have either four or eight neighbors according to the connectivity rules selected. (C) Boundary-searching algorithm using four-connectivity. The pixels marked with an 'X' are previously detected edge elements on the object boundary. Only three pixels need to be examined in order to find the next boundary element, using the criterion described in the text. The possible candidates, marked A, B and C, are searched for in a clockwise fashion. Note that this numbering arrangement will also work when rotated 90, 180 and 270°.

The four-connected rule, used in this study, requires that only three of the eight possible neighboring pixel positions need to be examined to find the next connected edge element according to the criterion above (Figs 4B and C). Examination of the three possible positions was conducted in a clockwise fashion, beginning with the previously detected edge element. This caused the boundary-following routine to move around the object in a clock-wise direction until it encountered the starting point. At this point the routine halted.

Connectivity rules used in determining the object boundary produce a tracing where each edge element is displaced by no more than one pixel (either higher or lower, to the right or left) from its neighbors. This condition can be used to produce a coding of the edge-map which describes the boundary as a series of one-pixel wide displacements in the X or Y direction.[6] Edge maps can then be used with various chain-coding routines to determine shape parameters such as area, perimeter or outline.[3,11,12]

In this study we used the edge-map to calculate statistics of area and perimeter describing the shape of the chloroplast from which the digital

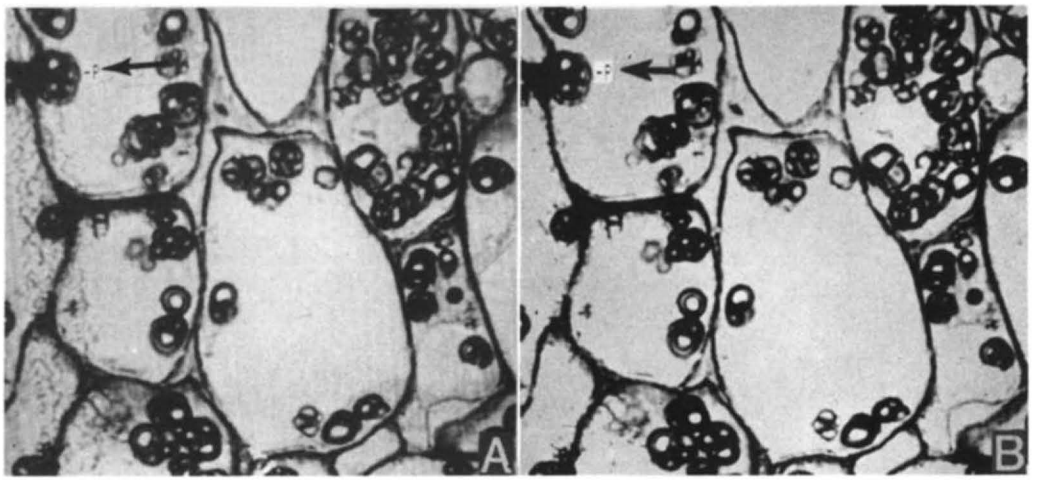

FIG. 2. Digital image of *C. esculenta* tissue (A) demonstrating the sharp contrast between chloroplast, cell wall and background regions, and (B) showing a digital image of Fig. 2A after a threshold procedure was used to suppress variations in background intensity. All pixels with a gray value above an arbitrary threshold were assigned new gray values equal to the average background intensity. Arrows denote computer-generated label of plastid. × 625.

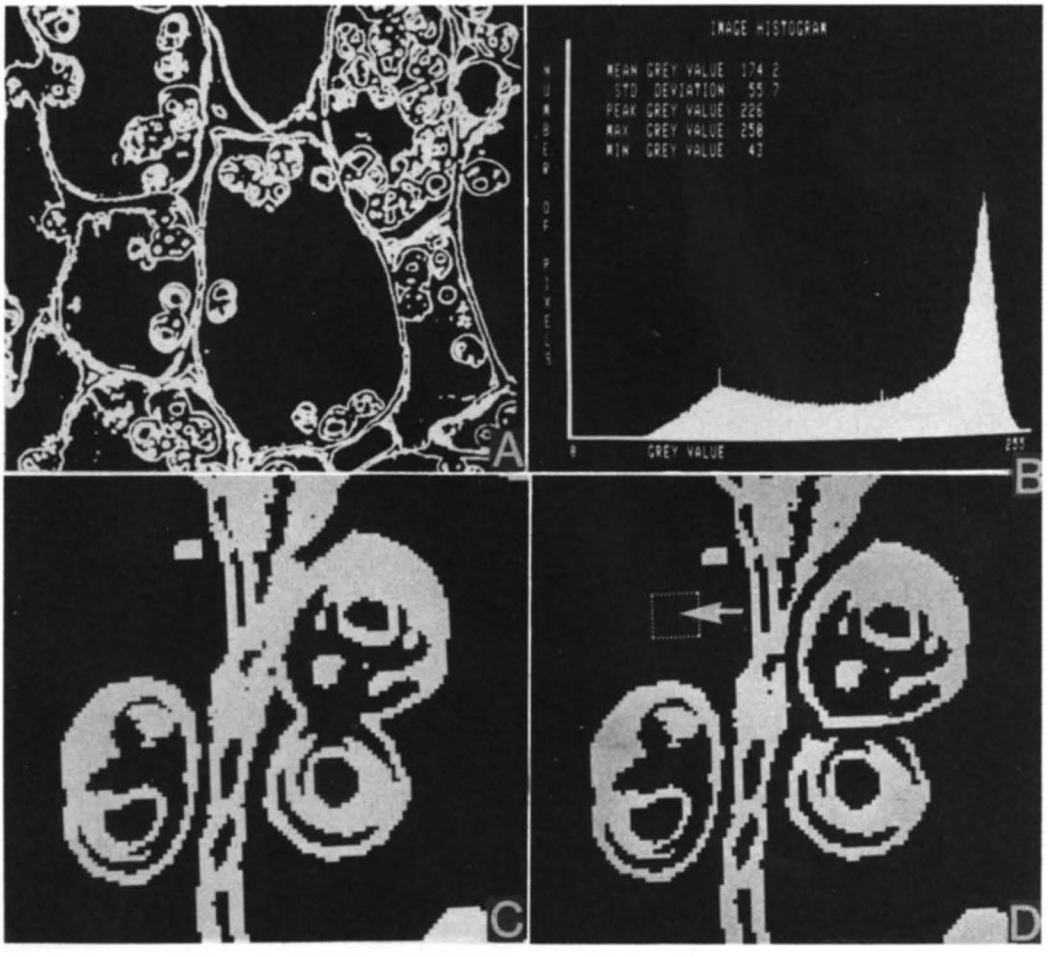

FIG. 3. Digital image of Fig. 2 after the threshold procedure. (A) The resulting image contains only two gray values, white and black. × 625. (B) Gray value histogram of the image in Fig. 2. This histogram contains two peaks which can be used to determine the gray value threshold. The peak on the left is created by areas of the image containing chloroplasts or cell wall, whereas the one on the right is created by background areas. A threshold value between the two peaks will separate these two areas in the digital image. (C) Merging of cell wall and chloroplast due to incomplete gray value separation. × 1900. (D) Separation of cell wall and chloroplast through manual outlining. The image in Fig. 3C was edited to separate the chloroplast from the adjacent cell wall. Area and perimeter of the isolated chloroplast were then calculated as shown in the figure. An example of a computer-generated box (arrow) which can be moved by a joy-stick and allows for editing of the image is shown. × 1900.

image was made. These statistics were calculated while the edge-map was being generated, so that they were determined as quickly as the boundary-following routine could be completed. The calculated area and perimeter of each measured chloroplast was independent of the starting position of the boundary-following procedure.

DISCUSSION

Use of a computer-based morphometric technique to measure plant organelles has the advantages of greatly increasing the speed of analysis, and improving reliability. Successful application of this technique requires high quality images with good contrast, within which objects of interest can be separated from background areas by their gray value differences.

When objects cannot be fully identified by differences in gray value, or when the distribution of these values within an object is large, the position of the threshold may be difficult to determine.[18,19] Uncertainty regarding the threshold can introduce errors in the determination of object size, particularly when these thresholds are determined interactively. Several automated procedures, based solely on features of the gray value histogram,[1,18] have been proposed for determining these thresholds.

Uncertainty in the determination of the gray value threshold did not greatly influence the shape parameters measured during this study. This conclusion is based on two observations regarding area and perimeter: (1) repeated measurements of a single chloroplast which involved a redefinition of the threshold did not significantly alter the measured values, and (2) measurements obtained by manual outlining of chloroplasts in the digital image produced values similar to those determined automatically with the threshold technique. The insensitivity of these morphometric measurements to the threshold selection step was influenced primarily by the high contrast of the tissue images (Figs 2 and 3). A similar conclusion was reached on the basis of findings that the size and shape of inclusions in sectioned lung tissue could be measured reproducibly as a consequence of high image contrast.[14]

The accuracy of automated morphometric techniques can also be affected by sources of distortion within the optical and video imaging systems. Most video camera systems show some degree of shading distortion, typically reported by the manufactures at 5–20%. This results in a change in light sensitivity across the face of the video tube, and can influence the gray value of a digitized object depending on its position in the field.[5] Such position-dependent differences can introduce errors in morphometric measurements when gray value thresholding techniques are used. This source of distortion can be minimized by using (1) video cameras selected for low shading distortion, (2) only high contrast images, and (3) utilizing digital shading correction routines when necessary.[2,17] Shading distortion did not contribute to the measurements described here due to high image contrast and the use of a video camera with a built-in shading-correction circuit.

Another potentially serious source of error in an optical-video camera relates to the precision with which the rectangular scan across the tube face is reproduced. The quality of reproduction affects the optical image projected onto its surface. Errors in the scanning pattern produce geometric distortion in the image that can alter the apparent size and shape of objects, particularly towards the edges of the field. Distortion can be compensated for by (1) employing high-quality cameras with low inherent distortion, (2) restricting measurements to the center of the field where distortion is lowest, and (3) using digital 'warping' routines.[2,5,17]

Center-to-edge distortion was negligible in this study, due primarily to the use of a high-quality camera. There was, however, an unequal magnification in the image due to mismatching between the aspect ratio of the camera and the image processor. This mismatch has been corrected in previous studies by using a warping routine.[2] The source of distortion was found to be approximately 5% during this study, and was corrected by using separate horizontal and vertical calibration factors to calculate object size.

The large size of plant cells and their highly refractive nature make them ideal subjects for the types of morphometric analysis described here. Image analysis systems are becoming more and more common in the biological laboratory[8,15] and are being put to many innovative uses as new

applications of these machines are being discovered.

Acknowledgements—Supported in part by USDA cooperative research grant No. 12-14-5001-259, and the National Institutes of Health Grant RRO 1192. We thank Drs Peter van Schaik and Brent Tisserat for their interest.

REFERENCES

1. Abdou I. E. and Pratt W. K. (1979) Quantitative design and evaluation of enhancement/thresholding edge detectors. *Proceedings of the IEEE* **67,** 753–763.
2. Altar C. A., Walter R. J., Jr., Neve K. A. and Marshal J. F. (1984) Computer-assisted video analysis of [^{3}H]-spiroperidol binding autoradiographs. *J. Neurosci. Meth.* **10,** 173–188.
3. Bowie J. E. and Young I. T. (1977) An analysis technique for biological shape—III. *Acta Cytologica* **21,** 739–746.
4. Bradbury S. (1983) Commercial image analyzers and characterization of microscopical images. *J. Microscopy* **131,** 203–210.
5. Castleman K. R. (1979) *Digital image processing.* Prentice-Hall, Englewood Cliffs, N.J.
6. Cedenberg R. T. L. (1979) Chain link coding and segmentation for raster scan devices. *Computer Graphics Image Processing* **10,** 224–234.
7. Healey P. L., Michaud J. D and Arditti J. (1980) Morphometry of orchid seeds—III. Native California and related species of Goodyera, Piperia, Plantanthera and Spiranthes. *Am. J. Bot.* **67,** 508–518.
8. Inoue S. (1985) *Video microscopy.* Plenum Press, N.Y.
9. Nyman L. P. and Dengler N. (1978) Cell enlargement during leaf development of *Catharanthus roseus. Canad. J. Bot.* **56,** 592–605.
10. Nyman L. P., Gonzalez C. J. and Arditti J. (1983) *In-vitro* selection for salt tolerance of Taro (*Colocasia esculenta*, var. *antiquorum*). *Ann. Bot.* **51,** 229–236.
11. Olson A. C., Larson N. M. and Hechman C. A. (1980) Classification of cultured mammalian cells by shape analysis and pattern recognition. *Proc. Natn. Acad. Sci. (U.S.A.)* **77,** 1516–1520.
12. Pavlidis T. (1978) A review of algorithms for shape analysis. *Computer Graphics Image Processing* **7,** 243–258.
13. Pratt W. K. (1978) *Digital image processing.* Wiley, N.Y.
14. Rigaut J. P., Berggren P. and Robertson B. (1983) Automated techniques for the study of lung alveolar sterological parameters with the IBAS image analyser on optical microscopy sections. *J. Microscopy* **130,** 53–61.
15. Sklansky J., Sankar P. and Walter R. (1986) Biomedical image processing. In T. S. Young and K. S. Fu, eds. *Handbook of image processing.* Academic Press, N.Y.
16. Walter R. J. and Berns M. W. (1981) Computer-enhanced video microscopy: digitally processed images can be produced in real time. *Proc. Natn. Acad. Sci. (U.S.A.)* **78,** 6927–6931.
17. Walter R. J. and Berns M. W. (1986) Digital image processing. In Shinya Inoue, ed. *Video microscopy.* Plenum Press, New York,
18. Weszka J. S. (1978) A survey of threshold selection techniques. *Computer Graphics Image Processing* **7,** 259–265.
19. Weszka J. S. and Rosenfeld A. (1979) Histogram modification for threshold selection. *IEEE Trans. on Systems, Man and Cybernetics* **9,** 38–52.